Two-photon fluorescence of Coumarin 30 excited by optimally shaped pulses

Milan P. Poudel,[1,*] Alexandre A. Kolomenskii,[1,2] and Hans A. Schuessler[1]

[1]Department of Physics, Texas A&M University, College Station, Texas 77843-4242, USA

[2]a-kolomenski@physics.tamu.edu

*Corresponding author: milan.poudel@utsouthwestern.edu

Received 23 December 2009; revised 22 April 2010; accepted 1 May 2010; posted 3 May 2010 (Doc. ID 121978); published 26 May 2010

We optimized the two-photon fluorescence (TPF) of a Coumarin 30 dye by using a feedback-controlled femtosecond pulse shaping technique. For optimization we implemented an evolutionary algorithm with a liquid crystal phase-only pulse shaper in a folded 4f setup. The optimization procedure applied to the second harmonic generation, and TPF noticeably improved the output signals and demonstrated good convergence. In addition, signal ratios involving TPF and second harmonic generation (SHG) were successfully optimized. The correlation between TPF and SHG was studied, and it was found to decrease when the pulse shape was close to the optimum. These experimental results are of interest for potential applications of coherent control to complex molecular systems as well as in biomedical imaging.

OCIS codes: 320.5520, 320.5540, 350.5030, 190.7110.

1. Introduction

Adaptive femtosecond coherent control has proved to be an efficient tool for optimization of different physical processes [1–4]. In this approach, active feedback is used to iteratively optimize a molecular process by manipulating the spectral components of the femtosecond laser pulses. Since its introduction by Judson and Rabitz [5], there has been a rapid growth of experimental studies with this technique for solving optimization problems of complex systems. By now, it is widely used in different processes, including, for example, adaptive pulse compression in a dispersive medium [6], molecular electronic population transfer [7], high harmonic generation [8], two-photon absorption [9], and energy conversion in light harvesting molecules [10].

For ultrashort laser pulses, two-photon transitions are induced by pairs of photons of a laser pulse for which the sum of the two-photon energies equals the energy of the transition. The probability of a molecule to absorb two photons simultaneously is proportional to the square of the intensity of the input beam [11,12]. Consequently, for low intensities this two-photon excitation process is usually weaker compared to the one-photon excitation. However, temporal compression of the pulse and the simultaneous increase of the intensity tend to increase the two-photon excitation and the accompanying fluorescence. In the following text we will refer to these two related processes as simply two-photon fluorescence (TPF).

TPF excitation has a broad range of applications in laser spectroscopy as well as in the imaging of biosystems [3]. Two-photon excitation also allows reaching molecular states with twice the energy of the incident photons, thus enabling fluorescence studies in a shorter wavelength region with visible and IR radiation.

Early on, Meshulach and Silberberg investigated two-photon transitions in Cs gas [9]. With femtosecond pulse shaping, Brixner *et al.* controlled the multiphoton molecular excitation of a charge-transfer coordination complex dissolved in methanol [13].

0003-6935/10/163075-07$15.00/0

Hornung *et al.* have shown the optimization of a two-photon transition for Na [14].

In this paper, we have optimized the two-photon excitation of Coumarin 30 dye molecules in a methanol solution with adaptively shaped femtosecond laser pulses. The optimization is achieved by implementing a feedback-control pulse shaping technique. By using the term "optimization," we refer to the maximization of the respective signal employed in the feedback loop.

The Coumarin 30 molecule has a large two-photon absorption cross section around 800 nm and a high single-photon fluorescence quantum yield in the visible region around 500 nm, which makes it suitable for use as a colorant, a dye laser medium, and as a nonlinear optical medium for imaging [15]. It also has several biological applications and was described as a potential agent for cancer treatment and as an anticoagulant [16].

2. Experiment

The experimental setup is shown in Fig. 1. The femtosecond laser pulse formed by an oscillator and a regenerative amplifier was sent to a liquid crystal (LC) pulse shaper, which controlled the phases $\beta(\omega_i)$ of the spectral components with frequencies ω_i.

The spectral phase $\beta(\omega)$ is presented in a polynomial form

$$\beta(\omega) = \beta_0 + \beta_1(\omega - \omega_0) + \frac{1}{2}\beta_2(\omega - \omega_0)^2 + \frac{1}{6}\beta_3(\omega - \omega_0)^3 + \frac{1}{24}\beta_4(\omega - \omega_0)^4 + \ldots, \quad (1)$$

where ω_0 is the central frequency, β_0 and β_1 determine a phase shift and a temporal shift, respectively, and $\beta_k (k = 2 - 4)$ represent the second-, third-, and fourth-order dispersion coefficients responsible for the variation of the pulse shape. These dispersion coefficients were used as control parameters, and their optimal values, and, therefore, the optimal phases of the spectral components, were then sought through the adaptive feedback process based on an evolutionary algorithm [17].

Instead of the traditional scheme with symmetric beam paths before and after the grating and the modulator, we employed a scheme in folded geometry with an end mirror immediately after the spatial light modulator (SLM), as shown in Fig. 2. This setup is intrinsically highly symmetric and can be readily aligned.

An additional advantage is that it produces twice the phase shift of an unfolded setup, due to a double passage through the modulator. A grating with 1800 grooves/mm, a concave spherical mirror with a focal length of 50 cm, and a cylindrical lens with a focal length of 10 cm were used for spectrally dispersing (at the input) and recollimating (at the output) the laser pulses. A laser pulse with a spatially dispersed spectrum passed the LC matrix with 640 pixels in the SLM (SLM-640, JenOptik). The control of the laser pulse shape was achieved by applying a specific voltage to each pixel of the LC matrix and, in this way, modulating the phases of the spectral components. After reflection on the end mirror, the pulse was reassembled by propagating it back with its output direction slightly shifted relative to the input pulse. Because only the phases of spectral components were modulated in this study, the spectral amplitude and the total pulse energy were practically unchanged during the optimization process [9].

The output pulse from the shaper was divided by a beam splitter. One subbeam was focused using a 200 mm lens on a cuvette containing a 1 mM aqueous solution of Coumarin 30, and the emitted TPF signal was filtered optically and detected by a photomultiplier (PMT). The other subbeam was focused on a beta barium borate crystal to produce the second harmonic, which was filtered and detected by a photodiode. A mechanical chopper with a 500 Hz modulation frequency synchronized the laser pulse repetition rate of 1 kHz, so that the pulses were alternatively transmitted and blocked to enable background subtraction. The signal was detected with a lock-in amplifier

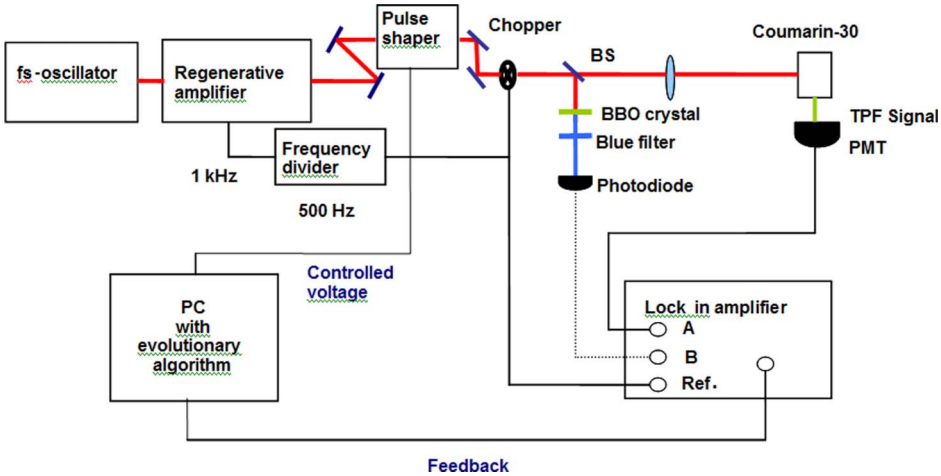

Fig. 1. (Color online) Schematic diagram of the experimental setup.

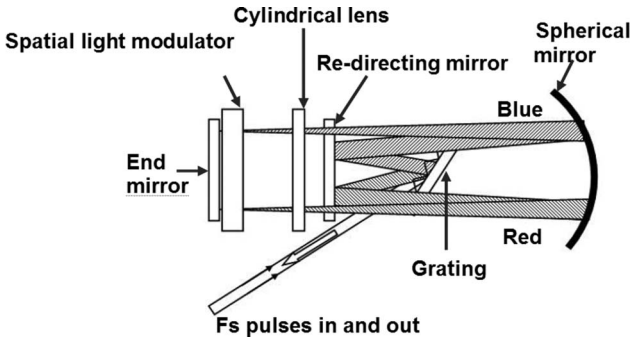

Fig. 2. Schematic diagram of folded 4*f* setup (top view).

referenced to the chopper, thus implementing narrow band detection. Figure 3 shows the chemical structure as well as the absorption and emission spectra of a Coumarin 30 molecule.

The key role in the feedback-control experiment is played by an evolutionary algorithm. In the implemented algorithm [17], one generation uses 48 individuals (vectors of voltages on the pixels of the LC matrix) and the fitness value is measured for every individual. The latter is determined by the signal under optimization. A new generation is built from the previous by combining parents (the fittest individuals), producing mutations (changes of the vector elements by some random values) and crossovers (recombination of elements of two vectors) to provide optimal convergence. By successive repetition of this scheme, individuals with the highest fitness values are selected, and they produce better offspring for subsequent generations, until the maximum output value is reached. Typically, convergence was achieved after 15 to 20 generations. Convergence strongly depended on the laser output fluctuations, which were minimized for better performance.

3. Results

In different experiments, we optimized the second harmonic generation (SHG), TPF, the ratio between TPF and SHG (TPF/SHG), the ratio of TPF and laser

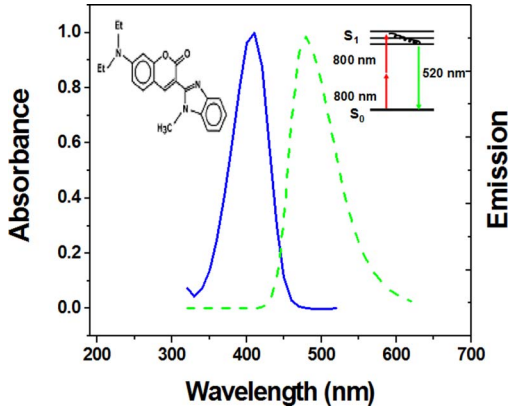

Fig. 3. (Color online) Normalized absorption and emission spectra of Coumarin 30 shown by the solid and dashed curves, respectively. The insets show the chemical structure of the Coumarin 30 molecule and schematic of TPF transitions.

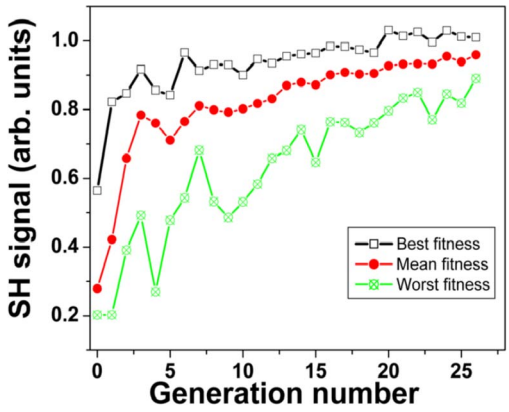

Fig. 4. (Color online) Convergence curves for optimization of the SHG signal. Three different curves show the best, worst, and mean SHG values.

power, and also $[(\mathrm{TPF})^2/\mathrm{SHG}]$. In addition, we performed a correlation analysis between the TPF and SHG signals.

A. Optimization of Second Harmonic Generation and Two-Photon Fluorescence

In the optimization of the SHG signal, starting from the initial pulse of duration $\tau = 45$ fs, the optimization resulted in a nearly transform-limited pulse with a duration of $\tau = 33$ fs, producing a significant increase in the SHG signal. Figure 4 shows the evolution of the second harmonic signal during optimization. In each optimization run, the best, worst, and mean SHG values were recorded. In Fig. 4 the best fitness signal gradually comes to saturation. The signals from the mean and worst individuals for each generation are still improving, while the best fitness signal starts fluctuating around the same level. This shows that the optimal parameters have been already achieved, and the fluctuations are related to inevitable variations due to fluctuations of the laser parameters and noise. Figure 5 depicts the spectrally and time-resolved images of the pulses obtained before and after the optimization. The pulses were measured with GRENOUILLE, a device based on the frequency-resolved optical gating technique with SHG [18]. It uses VideoFROG software (Mesa Photonics), which includes a retrieval algorithm, calculating

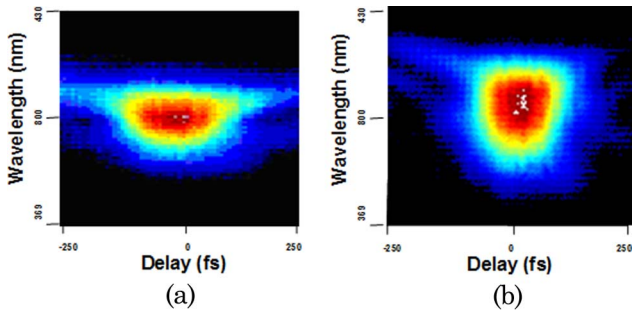

Fig. 5. (Color online) Pulse images from GRENOUILLE: (a) before (pulse duration $\tau = 45$ fs) and (b) after ($\tau = 33$ fs) the optimization of the SHG signal.

the pulse duration from the measured intensity distribution.

Figure 6 shows the detected spectra before and after optimization of the TPF intensity. In this process the TPF signal increased about twofold. The fluorescence spectral interval used for optimization extended from 480 to 530 nm at FWHM.

During optimization, all four dispersion parameters of Eq. (1) are determined. The fluorescence emission quickly increases in the first few generations and nearly saturates after 10 to 12 generations. In Fig. 7, normalized second-, third-, and fourth-order phase dispersion coefficients (β_2, β_3, and β_4) are plotted versus the generation number. In our algorithm, the set of dispersion coefficients was optimized within the following ranges: for the second order, $\pm 200\,\mathrm{fs}^2$; for the third order, $\pm 40000\,\mathrm{fs}^3$; and for the fourth order, $\pm 300000\,\mathrm{fs}^4$. The graph in Fig. 7 shows a rather quick convergence of the dispersion coefficients in the optimization process. The convergence in different runs was quite reproducible; however, the final values of the coefficients could slightly vary.

B. Optimization of (TPF/SHG) Ratio

As shown above, when starting with a relatively long pulse, both types of optimization (TPF and SHG) lead to shortening the optimized pulse. To explore a possible difference, we performed an optimization with the goal of achieving the maximum ratio of TPF to SHG. The idea behind this optimization goal is to cancel the dominating effect of the nonlinear excitation, because it is present in both numerator and denominator of this ratio. The possibility of controlling the ratio (TPF/SHG) would indicate that the two processes can be distinguished by adaptive pulse shaping [13].

During this optimization, signals of both the ratio and the fluorescence were increased, while the SHG signal initially increased significantly and then stayed nearly the same, only slightly decreasing, as shown in Fig. 8. In this process, the pulse duration changed from 45 fs (initial) to 34 fs (final).

To investigate the chirp of the optimal pulse, we varied the parameter of the second-order dispersion

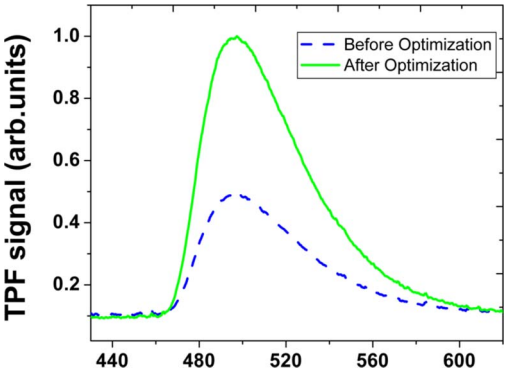

Fig. 6. (Color online) TPF spectra of Coumarin 30 measured before optimization (dashed curve) and after optimization (solid curve).

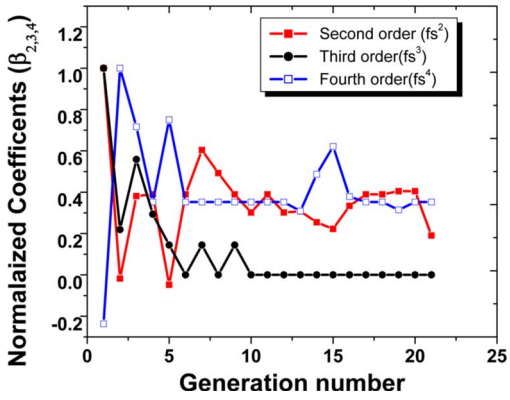

Fig. 7. (Color online) Typical convergence of the second-, third-, and fourth-order dispersion coefficients for TPF optimization.

in small steps by using the SLM LC matrix and also the Dazzler (Fastlite)[19] in two independent series of experiments. We came to the conclusion that the absolute value of the chirp for the optimal pulse was less than about $50\,\mathrm{fs}^2$ for our experimental parameters. Because of the small value of this chirp, its sign could not be determined.

C. Optimization of Ratio $[(\mathrm{TPF})^2/\mathrm{SHG}]$

When starting optimization with a pulse that is far from the optimal, both processes of optimization for TPF and SHG follow similar trends of pulse shortening. Under conditions when the noise is high or the signal channels for TPF or SHG are not ideally linear, the optimization of the ratio [(TPF)/ SHG] may still take place but lead to a false optimization solution.

To avoid this problem, we performed an optimization with another goal, namely, the ratio of the square of the fluorescence to the second harmonic signal $[(\mathrm{TPF})^2/\mathrm{SHG}]$. During this optimization, the ratio increased significantly, and the process was also accompanied by optimization of the TPF signal, as shown in Fig. 9, allowing us, at the same time, to discriminate optimal pulses for TPF and SHG. In the final stage of this optimization, the signals of both the ratio and the fluorescence were increasing while the SHG signal was decreasing.

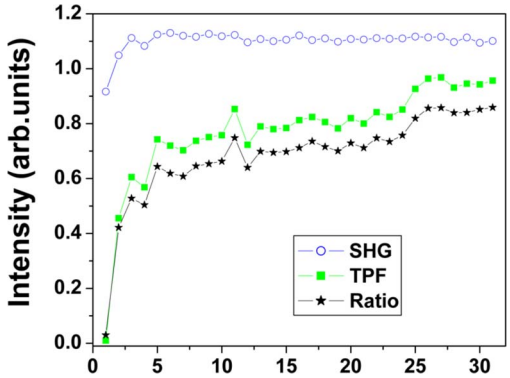

Fig. 8. (Color online) Evolution of TPF, SHG, and their ratio during (TPF/SHG) optimization.

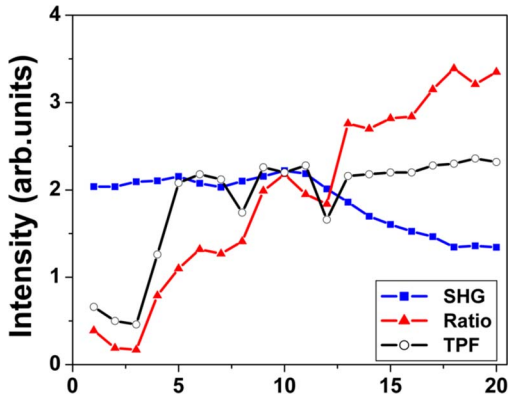

Fig. 9. (Color online) TPF, SHG, and their ratio $[(\mathrm{TPF})^2/\mathrm{SHG}]$ during optimization of the latter.

4. Measurements of Correlations between Two-Photon Fluorescence and Second Harmonic Generation Signals

We have also investigated the correlation between TPF and SHG signals. It characterizes how closely these signals follow each other for different realizations (individuals) of the excitation pulses. The normalized correlation function $G_{\mathrm{norm}}(\Delta N)$ is defined as [20]

$$G_{\mathrm{norm}}(\Delta N) = \frac{\langle \partial I_1(N)\partial I_2(N+\Delta N)\rangle}{\sqrt{[\langle \partial I_1^2(N)\rangle \langle \partial I_2^2(N)\rangle]}}, \qquad (2)$$

where $\partial I_1(N) = I_1(N) - \langle I_1\rangle$ and $\partial I_2(N+\Delta N) = I_2(N+\Delta N) - \langle I_2\rangle$ are the variations of the second harmonic and fluorescence signals, respectively, and $\langle\rangle$ means averaging: $\langle I\rangle = N_{\max}^{-1}\sum_{N=1}^{N_{\max}} I_N$. In these expressions, N is the sequential number of an individual realization of the pulse shape that is used in the trial and, correspondingly, $\partial I_1(N)$ and $\partial I_2(N)$ present two sequences of values with the running number N; ΔN is the shift of this number, and $N_{\max} \gg 1$ is the total number of individuals in the selection, used for the correlation analysis.

In the process shown in Fig. 10(a), the SHG signal was optimized, while both the TPF and the SHG outputs were measured. The data from Fig. 10(a) are divided into two portions: one is the initial stage with data points in the range ($N = 300$–900), and the other one (data points $N = 900$–1900) is the final stage of the optimization process. We used the second portion for producing the correlation function in Fig. 10(b). The correlation function was calculated using MATLAB. During optimization the pulse shapes were varied, resulting in variations of the TPF and SHG signals, which can be clearly seen in Fig. 10(a). When the optimization reaches a plateau, these variations correspond to a relatively small deviation of the pulse from the optimal one. With these conditions, the difference between TPF and SHG in the normalized correlation function becomes more noticeable. The middle peak (the shift $\Delta N = 0$) confirms that the two phenomena are highly correlated. However, the maximum value of the correlation function is less than 1 by $\delta = 0.23$, as shown in Fig. 10(b). For the portion of the data corresponding to the initial stage of the optimization process (data points $N = 300$–900), the deviation $\delta = 0.08$, and it is less than for the portion of the data corresponding to the final stage of the optimization. Thus, the maximum of the normalized correlation function has the trend of decreasing during the optimization, and the deviation from 1 quantifies the difference in the optimization of the two processes.

To assess the influence of noise on the correlation function, the beam of the second harmonic was split into two subbeams, which were detected in the two measuring channels of the same setup, and then the correlation function of the signals from these two channels was calculated. In this measurement we obtained the higher values of correlation with $\delta = 0.06$, as shown in Fig. 10(c). The noise level of the TPF signal was similar to that of the SHG signal. The smaller reductions of the correlation function for measurements of the same signal (SHG or TPF) in both detection channels, compared to the reduction in correlation of the TPF and SHG signals, demonstrated that the influence of noise was small, and the deviation δ in Fig. 10(b) is mainly due to the different optimal realizations for the two processes.

The larger reduction of the correlation between TPF and SHG signals confirms that these two processes are maximized by different pulses. The smaller peaks of the correlation function, noticeable in

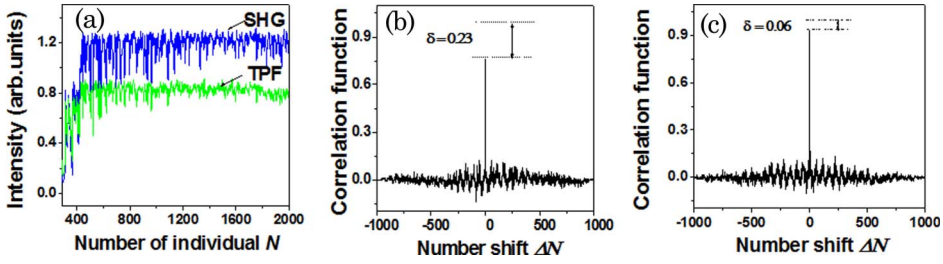

Fig. 10. (Color online) Correlation analysis of the signals: (a) TPF and SHG signals for all individuals while SHG is optimized; (b) correlation between TPF and SHG (the deviation of maximum of the correlation function from 1 by $\delta = 0.23$ is due to both the different nature of the two processes and the noise); and (c) correlation function of the SHG signals measured by two detection channels—in this case, the deviation of the maximum from 1, $\delta = 0.06$, is due to noise, and it is smaller than in Fig. 10(b), showing a relatively small influence of the noise.

Figs. 10(b) and 10(c), correspond to multiples of the number of individuals in one generation. Because each generation also contains individuals that are relatively far from the optimal one, the correlation of the TPF and SHG signals experiences spikes with period 48, equal to the number of individuals in a generation.

5. Discussion

By using the feedback-control pulse shaping technique, we were able to increase the TPF signals significantly. The optimization of TPF was also investigated previously in other molecular systems [3,4]. For the dye molecules LD690 and LDS750, a positively chirped pulse increased the total amount of the single-photon fluorescence [7]. In this case, the positive chirp pulse was found to be favorable, because the increase in time frequency of the positively chirped pulse leads to sequentially populating higher and higher energy levels and also prevents dumping back excited states by stimulated transitions. Lee *et al.* [21] have shown that two-photon emission efficiency of DCM dye was optimized with negatively chirp pulses, which they describe in terms of the wave packet localization in the excited states.

In our experiments with Coumarin 30 dye, we found that a near-transform-limited pulse was most favorable for the enhancement of TPF. Because transform-limited pulses maximize the SHG process [6,21], the pulse shapes optimal for TPF and SHG should be quite close in our case. Our experiments with several different optimization goals demonstrated the possibility of adapting the pulse shape to electronic and vibrational properties of the molecule in such a way that a given ratio of the signals is optimized. By optimizing the ratio (TPF/SHG), we could exclude the intrinsic nonlinear intensity dependence for these two-photon processes.

Although we could not measure the difference of the optimal pulses for the TPF and the SHG by directly optimizing these processes, we could see different behavior of these signals for the ratios, [TPF/SHG] and [TPF^2/SHG], as optimization goals. This confirms that the two processes are optimized by different pulse shapes. Although the latter differ only slightly, this difference manifests itself in the correlation measurements, showing the sensitivity of this approach to small differences in the responses. Correlation analysis shows that the TPF and SHG signals are highly correlated, because both processes tend to be optimized by shorter pulses. However, the different nature of these two processes leads to a decrease of correlation with the progress of the optimization process, making subtle differences noticeable.

6. Conclusion

In this research, we designed and implemented a pulse shaper with a folded 4f configuration. We have demonstrated that TPF can be increased noticeably by a pulse shaping technique with an evolutionary algorithm. With different optimization goals, i.e., (TPF/SHG) and [$(TPF)^2$/SHG], it was possible to remove the trivial intensity dependence, or alternatively, enhance the role of one of the processes (TPF) in the optimization. The successful optimization of these ratios shows the effectiveness of the feedback-control pulse shaping for steering the excitation of electronic and vibrational motions of a molecule to achieving the desired goal. The introduction of a new optimization function [$(TPF)^2$/SHG] improves the convergence of the optimization process under noisy conditions.

The performed correlation analysis shows that two-phenomena TPF and SHG are highly correlated. The correlation is higher during the initial stages of the optimization and decreases when the pulse approaches the optimal shape, which is different for each of these processes. These experimental results are of interest for potential applications in chemical physics as well as in biomedical imaging.

We are thankful to Alvin Yeh and Hartmut Schroeder for reading the manuscript and for their valuable suggestions. This work was partially supported by the Robert A. Welch Foundation (grant A1546), the National Science Foundation (NSF) (grants 0722800 and 0555568), and the Air Force Office of Scientific Research (grant FA9550-07-1-0069).

References

1. T. Brixner and G. Gerber, "Quantum control of gas-phase and liquid-phase femtochemistry," Chem. Phys. Chem. **4**, 418–438 (2003).
2. M. Roth, L. Guyon, J. Roslund, V. Boutou, F. Courvoisier, J. Wolf, and H. Rabitz, "Quantum control of tightly competitive product channels," Phys. Rev. Lett. **102**, 253001 (2009).
3. I. Pastrik, E. J. Brown, Q. Zhang, and M. Dantus, "Quantum control of the yield of a chemical reaction," J. Chem. Phys. **108**, 4375–4378 (1998).
4. I. Otake, S. S. Kano, and A. Wada, "Pulse shaping effect on two-photon excitation efficiency of α-perylene crystals and perylene in chloroform solution," J. Chem. Phys. **124**, 014501 (2006).
5. R. Judson and H. Rabitz, "Teaching laser to control molecules," Phys. Rev. Lett. **68**, 1500–1504 (1992).
6. D. Yelin, D. Meshulach, and Y. Silberberg, "Adaptive femtosecond pulse compression," Opt. Lett. **22**, 1793–1795 (1997).
7. C. J. Bardeen, V. V. Yakovlev, K. R. Wilson, S. D. Carpenter, P. M. Weber, and W. S. Warren, "Feedback quantum control of molecular electronic population transfer," Chem. Phys. Lett. **280**, 151–158 (1997).
8. R. Bartels, S. Backus, E. Zeek, L. Misoguti, P. Vdovin, I. Chistov, M. Murname, and H. Kapteyn, "Shaped-pulse optimization of coherent emission of high-harmonic soft-x-rays," Nature **406**, 164–166 (2000).
9. D. Meshulach and Y. Silberberg, "Quantum control of multiphoton transitions by shaped ultrashort optical pulses," Nature **396**, 239–242 (1998).
10. J. L. Herek, W. Wohleben, R. Cogdell, D. Zeidler, and M. Motzkus, "Quantum control of energy flow in light harvesting," Nature **417**, 533–535 (2002).
11. M. Kauert, P. C. Stoller, M. Frenz, and J. Ricka, "Absolute measurement of molecular two-photon absorption cross-sections using a fluorescence saturation technique," Opt. Express **14**, 8434–8447 (2006).

12. J. Strohaber, M. P. Poudel, A. A. Kolomenskii, and H. A. Schuessler, "Single snapshot and intensity-resolved two-photon fluorescence measurements," Opt. Lett. **35**, 22–24 (2010).
13. T. Brixner, N. H. Damrauer, B. Kiefer, and G. Gerber, "Liquid-phase adaptive femtosecond quantum control: removing intrinsic intensity dependencies," J. Chem. Phys. **118**, 3692–3701 (2003).
14. T. Hornung, R. Meier, D. Zeidler, K. L. Kompa, D. Porch, and M. Motzkus, "Optimal control of one- and two-photon transitions with shaped femtosecond pulses and feedback," Appl. Phys. B **71**, 277–284 (2000).
15. S. Santhilkumar, S. Nath, and H. Pal, "Photophysical properties of coumarin-30 dye in aprotic and protic solvents of varying polarities," Photochem. Photobiol. **80**, 104–111 (2004).
16. B. Kovac and I. Novak, "Electronic structures of coumarins," Spectrochim Acta Part A **58**, 1483–1488 (2002).
17. D. Zeidler, S. Frey, K. L. Kompa, and M. Motzkus, "Evolutionary algorithms and their application to optimal control studies," Phys. Rev. A **64**, 023420 (2001).
18. R. Trebino, K. W. Delong, D. N. Fittinghoff, J. N. Sweetser, M. A. Krumbugel, and B. A. Richman, "Measuring ultrashort laser pulses in the time-frequency domain using frequency-resolved optical gating," Rev. Sci. Instrum. **68**, 3277–3295 (1997).
19. F. Verluise, V. Laude, Z. Cheng, C. Spielmann, and P. Tournois, "Amplitude and phase control of ultrashort pulses by use of an acousto-optic programmable dispersive filter: pulse compression and shaping," Opt. Lett. **25**, 575–577 (2000).
20. M. O. Scully and M. S. Zubairy, *Quantum Optics* (Cambridge U. Press, 1997).
21. S. H. Lee, K. H. Jung, J. H. Sung, K. H. Hong, and C. H. Nam, "Adaptive quantum control of DCM fluorescence in the liquid phase," J. Chem. Phys. **117**, 9858–9861 (2002).